Compact Modeling of Doped Symmetric DG MOSFETs with Regional Approach

Karthik Chandrasekaran[*], Zhaomin Zhu[*], Xing Zhou[*], Wangzuo Shangguan[*], Guan Huei See[*], Siau Ben Chiah[*], Subhash C. Rustagi[**], and Navab Singh[**]

[*]School of Electrical & Electronic Engineering, Nanyang Technological University
Nanyang Avenue, Singapore 639798, exzhou@ntu.edu.sg
[**]Institute of Microelectronics, 11, Science Park Road, Singapore Science Park II, Singapore 117685

ABSTRACT

A compact model for the surface and mid-gap potentials of *doped* symmetric double-gate MOSFETs is presented. A unified regional approach is used to derive the model equations from Poisson equation. The fully-depleted double-gate MOSFET has four regions of operation, accumulation, depletion, weak or volume inversion, and strong inversion. The model is derived physically in all regions, with expressions for the flat-band, fully-depleted, and threshold voltages scalable over silicon channel doping and thickness, and unified to obtain a single-piece explicit model for the surface potential and mid-gap potential. The model has been verified in comparison with numerical device potentials, charges, and capacitances for various channel doping and thickness.

Keywords: compact modeling, regional surface/mid-gap potential, symmetric double-gate MOSFET, ultra-thin body, volume inversion

1 INTRODUCTION

Double-gate (DG) MOSFET is emerging as a device of choice for nanoscale CMOS due to reduced 2D short-channel effects (SCEs) such as drain-induced barrier lowering, a sharper subthreshold slope, better carrier transport, and more current drive or gate capacitance per device [1]. Such advanced devices are being fabricated in several configurations including planar, vertical, FinFET, and various other three-dimensional geometries [2]. MOSFET compact modeling for circuit simulation requires accurate and physics-based formulations and, in the mean time, computationally efficient. Models that have been proposed for these devices in principle lack computational efficiency since they rely on numerical iteration to solve the fundamental equations [3]. The existing DG MOSFET models consider the channel as *undoped*. Undoped symmetric double-gate (s-DG) MOSFETs have been solved both implicitly [4, 5, 8] and analytically [6, 7, 8], while undoped asymmetric cases have been solved implicitly in literature. Since analytic solutions offer both advantages of greater physical insight and efficiency than their iterative counterparts, an explicit analytic formulation is still highly desirable. In this paper, we propose an explicit analytic solution for the surface potential of doped-body s-DG devices with the regional approach.

2 DOPING ISSUE IN DG-MOSFET

The volume of a DG MOSFET channel is very small, so the number of atoms in the channel would be small if it is doped. The dopant could be distributed randomly at different locations in different devices. Hence, it could cause fluctuations in electrical characteristics due to the fluctuation in dopant locations. Therefore, doping of DG MOSFETs is not desired and usually not used. Unfortunately, there would always be a small unintentional doping during real process. Even a small unintentional doping ($\sim 10^{15}$ cm^{-3}) could cause a large shift in the surface potential. From compact-modeling point of view, the errors in surface potential due to ignoring doping can be on the order of *mili-volts*, which are unacceptable for compact models that are surface-potential based due to the exponential dependence in the drain current.

To observe the doping effect, an ideal uniformly-doped long-channel DG MOSFET is simulated using Medici. Figure 1 shows the shift in the surface potential from the undoped MOSFET at various doping levels. The shift in the level is due to the shift in the Fermi potential. Even if the surface potentials can be normalized to their own Fermi potentials and the gate voltage normalized with respect to the flat-band voltages, as would have been done in a model without considering doping, there is an mV error around the depletion region, which is due to the presence of the acceptor atoms, as shown in Fig. 2 when the difference in surface potential of a doped device with respect to the undoped device is plotted. This implies that a model for undoped DG device cannot be accurate in predicting surface potentials with (unintentional) doping variations.

Aside from practical considerations, one of the main reasons for ignoring doping in existing DG models is due to the mathematical difficulty, since the Poisson equation cannot be integrated twice when doping is included. In this paper, we formulate an explicit model for the *doped* symmetric-DG MOSFETs based on our unified regional approach to surface-potential/charge modeling [9], and demonstrate that this is a viable approach to unifying models for various types of emerging non-classical devices.

3 SURFACE POTENTIAL SOLUTION

In order to proceed to solve the surface potential explicitly, we start from the Poisson equation:

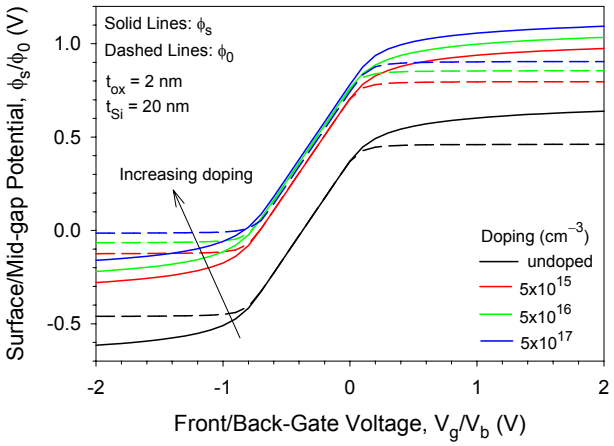

Figure 1: Surface and mid-gap potentials extracted from an ideal Medici s-DG device with (uniform) channel-doping variations and compared with the undoped device.

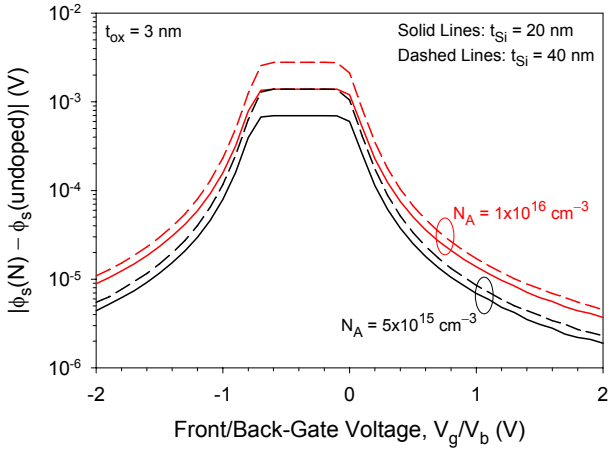

Figure 2: The difference between the surface potential of the doped device with the undoped one in Fig. 1 after normalizing to the respective Fermi potentials.

$$\frac{d^2\psi}{dx^2} = -\frac{\rho}{\varepsilon_{Si}} = -\frac{q\left(p - n + N_D - N_A\right)}{\varepsilon_{Si}} = \frac{q}{\varepsilon_{Si}}\left(n - p + N_A - N_D\right)$$
$$= \frac{q}{\varepsilon_{Si}}\left[n_i e^{(\psi-\phi_F-V_{cb})/v_{th}} - n_i e^{-(\psi-\phi_F)/v_{th}} + n_i e^{\phi_F/v_{th}} - n_i e^{-(\phi_F+V_{cb})/v_{th}}\right] \quad (1)$$
$$= \frac{qN_A}{\varepsilon_{Si}}\left[e^{(\psi-2\phi_F-V_{cb})/v_{th}} - e^{-\psi/v_{th}} + 1 - e^{-(2\phi_F+V_{cb})/v_{th}}\right]$$

In an s-DG MOSFET, the field in the middle of the channel ($x = x_0 = t_{Si}/2$ where t_{Si} is the silicon channel thickness) is always zero. Hence, the boundary condition for a (doped) s-DG MOSFET can be written as

$$\psi\big|_{x=x_0} = \phi_0, \quad \left.\frac{d\psi}{dx}\right|_{x=x_0} = 0 \quad \left(x_0 = t_{Si}/2\right). \quad (2)$$

where ϕ_0 is the "mid-gap" potential. By integrating (1) and applying (2), the surface ($x = 0$) electric field is given by

$$E_s^2 = \frac{2qN_A}{\varepsilon_{Si}}\left\{\begin{array}{l} e^{-(2\phi_F+V_{cb})/v_{th}}\left[v_{th}\left(e^{\phi_s/v_{th}} - e^{\phi_0/v_{th}}\right) - \left(\phi_s - \phi_0\right)\right] \\ +v_{th}\left(e^{-\phi_s/v_{th}} - e^{-\phi_0/v_{th}}\right) + \left(\phi_s - \phi_0\right) \end{array}\right\}. \quad (3)$$

From Gauss's law, the s-DG (input) voltage equation can be written as

$$V_g - V_{FB} - \phi_s = \mathrm{sgn}\left(\phi_s\right)\gamma\sqrt{f_\phi}$$
$$= \mathrm{sgn}\left(\phi_s\right)\gamma\sqrt{\begin{array}{l} v_{th}\exp\left(-\frac{2\phi_F + V_{cb}}{v_{th}}\right)\left[\exp\left(\frac{\phi_s}{v_{th}}\right) - \exp\left(\frac{\phi_0}{v_{th}}\right)\right] \\ +v_{th}\left[\exp\left(-\frac{\phi_s}{v_{th}}\right) - \left(-\frac{\phi_0}{v_{th}}\right)\right] \\ +\left(\phi_s - \phi_0\right) - \left(\phi_s - \phi_0\right)\exp\left(-\frac{2\phi_F + V_{cb}}{v_{th}}\right) \end{array}} \quad (4)$$

which approaches the conventional Pao–Sah voltage equation for bulk-MOS [10] when $\phi_0 = 0$. Hence, s-DG analysis is similar to analyzing an equivalent ultra-thin body (UTB) MOSFET for one half of the DG MOSFET.

The difference of ϕ_s and ϕ_0 can be expressed as

$$\phi_s - \phi_0 = \sqrt{2qN_A/\varepsilon_{Si}}\int_0^{x_0} f\left(\phi_s, \phi_0, \phi_F, V_{cb}\right)dx\,. \quad (5)$$

Combining (4) and (5), ϕ_s and ϕ_0 can be solved. But the second closed-form integral of Poisson equation in (5) is not possible. Most authors in literature solved the problem by considering only the case of undoped channels. We show below our unified regional (non-pinned) surface potential approach [9] to solving doped s-DG MOSFETs.

The DG MOSFET operation can be divided into four regions: accumulation, depletion, weak inversion (or volume inversion), and strong inversion. The potentials can be solved analytically in each region, and then smoothed using an interpolation function.

In the accumulation region, only the hole term can be considered. Then, we can integrate the Poisson equation twice to arrive at

$$\frac{q(\phi_s - \phi_0)}{2kT} = \ln\left[\cos\left(\frac{t_{Si}}{2}\sqrt{\frac{q^2N_A}{2\varepsilon_{Si}kT}}e^{-q\phi_0/2kT}\right)\right]. \quad (6)$$

ϕ_0 tends to be a constant when the gate voltage becomes negatively large. The minimum ϕ_0 [7] can be determined from (6)

$$\phi_{0\min} = -\frac{2kT}{q}\ln\left(\frac{\pi}{t_{Si}q}\sqrt{\frac{2\varepsilon_{Si}kT}{N_A}}\right). \quad (7)$$

We can see that $\phi_{0\min}$ is independent of oxide thickness. The unified mid-gap potential in the accumulation region is obtained by unifying (7) with the function $-(V_g - V_{FB})$. Once the mid-gap potential is determined, the surface potential in accumulation can be calculated from (6).

In the depletion region, when the channel is not fully depleted, the hole and electron terms can be considered negligible. When the channel is not fully depleted, the mid-gap potential is also zero (as in bulk):

$$\phi_0 = 0,\ e^{-2\phi_F/v_{th}}\left(e^{\phi_s/v_{th}} - e^{\phi_0/v_{th}}\right) \approx 0\,. \quad (8)$$

After applying the conditions specified in (8) to (4), we can calculate the surface potential in the depletion region using the formulation [9]

$$\phi_{s,sub} = \left[-\frac{\gamma}{2} + \sqrt{\frac{\gamma^2}{4} + V_g - V_{FB}} \right]^2 . \quad (9)$$

The depletion and accumulation pieces are unified using a square-root interpolation function [9].

In the weak (or volume) inversion region, the channel is completely depleted. The holes and (inversion) electrons can be considered negligible:

$$e^{-\phi_s/v_{th}} - e^{-\phi_0/v_{th}} \approx 0,\ e^{-2\phi_F/v_{th}} \left(e^{\phi_s/v_{th}} - e^{\phi_0/v_{th}} \right) \approx 0 . \quad (10)$$

The depletion charge is given by

$$Q_b = -qN_A \left(t_{Si}/2 \right) . \quad (11)$$

After applying (10) and (11) to (4) and (5), we can obtain

$$\phi_{s,vi} = V_g - V_{FB} - \frac{qN_A \left(t_{Si}/2 \right)}{C_{ox}} . \quad (12)$$

The mid-gap potential in the weak/volume inversion region can be calculated by applying full-depletion approximation

$$\phi_{0,vi} = \phi_{s,vi} - \frac{qN_A \left(t_{Si}/2 \right)^2}{2\varepsilon_{Si}} . \quad (13)$$

The onset of weak inversion is at the voltage where the channel is just fully depleted, which is given from Poisson solution by the expression

$$V_{FD} = V_{FB} + \frac{qN_A \left(t_{Si}/2 \right)^2}{2\varepsilon_{Si}} + \frac{qN_A \left(t_{Si}/2 \right)}{C_{ox}} . \quad (14)$$

The depletion and weak-inversion pieces are unified at the V_{FD} voltage using the same interpolation function as for the depletion and accumulation unification.

When the surface potential reaches twice the Fermi potential (i.e., at the "threshold voltage," V_t), the device operates in the strong-inversion region. In this region, a closed-form expression for the potential cannot be obtained when the acceptor and electron terms are both included in the equation. We use a full-depletion approximation to derive a relation between ϕ_s and ϕ_0 [11, 12]:

$$\phi_s - \phi_0 = \frac{qN_A \left(t_{Si}/2 \right)^2}{2\varepsilon_{Si}} . \quad (15)$$

When this approximation is used, the surface potential in strong inversion [9, 13] can be derived as

$$\phi_{s,str} = 2\phi_F + \Delta$$

$$\Delta = v_{th} \ln \left(a/b \right)$$

$$a = \frac{1}{\gamma^2} \left(V_g - V_{FB} - \phi^* \right)^2 \quad (16)$$

$$b = v_{th} \left\{ 1 - \exp \left[-\frac{1}{v_{th}} \left(\frac{qN_A \left(t_{Si}/2 \right)^2}{2\varepsilon_{Si}} \right) \right] \right\} .$$

The strong-inversion potential is then smoothed with the other surface potential pieces to give a unified regional surface-potential expression [14].

As will be seen, the key to physical parameter scalability lies in the physically-derived expressions for the "turning" voltages, V_{FB}, V_{FD}, and V_t, combined with the interpolation functions in the unified regional approach.

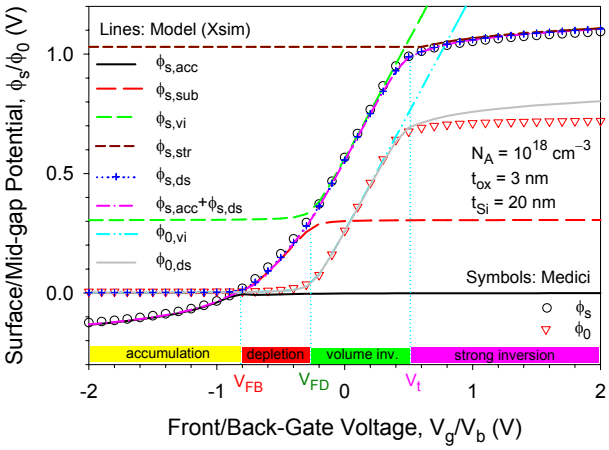

Figure 3: Regional and unified solution for the surface and mid-gap potentials of a doped symmmetric double-gate MOSFET, compared with the ideal Medici device.

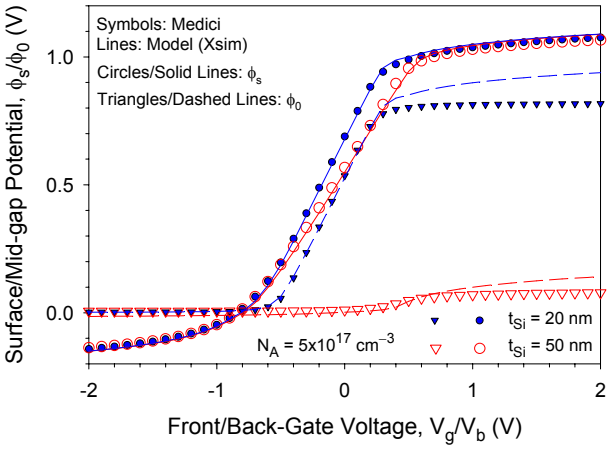

Figure 4: Scalability of the surface and mid-gap potentials for different channel thickness.

4 RESULTS AND DISCUSSION

Figure 3 shows the regional surface and mid-gap potential solutions from the model (lines) and Medici device (symbols). A high channel doping (10^{18} cm^{-3}) at 20-nm channel thickness is used to show the various behaviors, while the model physically scales with doping and channel thickness. The figure shows the regional accumulation, depletion, weak-inversion, and strong-inversion pieces. The transition from depletion to weak inversion is modeled physically by the fully-depleted voltage, V_{FD}. The strong-inversion piece is derived using a delta function (16), consistent with our bulk-charge formulation [9]. In the volume-/strong-inversion regions, the difference between ϕ_s and ϕ_0 is given by (15), which is the key to volume-inversion modeling. The small error in ϕ_0 in the strong-inversion region is due to this approximation; however, its effect on ϕ_s is negligible. Our model has a smooth transition from undoped to doped devices.

Figure 4 shows the scalability of the model for different channel thickness. As the channel thickness is increased to

larger than twice the maximum depletion width, the surface potential has a smooth transition to the bulk MOSFET model. The well predicted onset of volume inversion (at V_{FD}) for the t_{Si} = 50-nm device at a lower doping (5×10^{17} cm^{-3}), as compared to the one in Fig. 3 ($N_A = 10^{18}$ cm^{-3}, t_{Si} = 20-nm), can be clearly seen in Fig. 4 (open symbols).

Figure 5 shows the accurate prediction of the V_{FD} voltage for different channel doping, as compared with the ones extracted from Medici devices. The accuracy of the V_{FD} voltage is key to the modeling of the surface and mid-gap potentials in the unified regional approach.

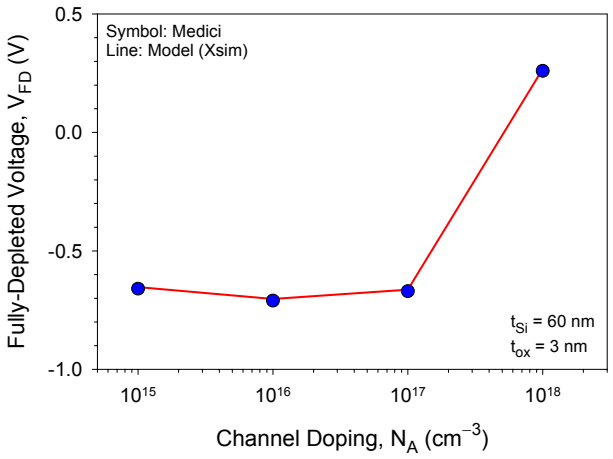

Figure 5: Prediction of the fully-depleted voltage (V_{FD}) for different channel doping, validated with those extracted from the corresponding Medici device.

5 CONCLUSION

A regional unified surface and mid-gap potential model has been derived for doped symmetric double-gate MOSFETs. The potentials have been derived regionally and unified using interpolation functions. The scalability of the model for different channel doping and thickness has been verified with numerical solutions. The approach demonstrates a first step towards unification of models for various types of devices, such as UTB, DG, bulk and SOI MOSFETs, with seamless transitions across doping levels and layer thicknesses.

Acknowledgement: This work was supported in part by the Institute of Microelectronics under Agreement for Research Collaboration HN/OCL/103/0105/IME through the A*STAR SERC Grant No. 042 114 0045, in part by the Semiconductor Research Corporation under Contract No. 2004-VJ-1166, and in part by the Nanyang Technological University under Grant RGM30/03.

REFERENCES

[1] Q. Chen, K. A. Bowman, E. M. Harrell, and J. D. Meindl, "Double jeopardy in the nanoscale court," *IEEE Circuits Devices Mag.*, vol. 19, no.1, pp. 28–34, Jan. 2003.

[2] J. P. Colinge, "Multiple-gate SOI MOSFETs," *Solid State Electron.*, vol. 48, pp. 897–905, 2004.

[3] Y. Taur, "Analytic solutions of charge and capacitance in symmetric and asymmetric double-gate MOSFETs," *IEEE Trans. Electron Devices*, vol. 48, pp. 2861–2869, Dec. 2001.

[4] Y. Taur, "An Analytical Solution to a double-gate MOSFET with undoped body," *IEEE Electron Device Lett.*, vol. 21, pp. 245–247, May 2000.

[5] J. He, X. Xi, C.-H. Lin, M. Chan, A. Niknejad, and C. Hu, "A Non-charge-sheet analytical theory of undoped symmetric double-gate MOSFETs from the exact solution of Poisson's equation using SPP approach," *Proc. NSTI WCM-Nanotech 2004*, Boston, vol. 2, pp. 124–127, 2004.

[6] Xuejie Shi and Man Wong, "Analytical solutions to the one-dimensional. oxide-silicon-oxide system," *IEEE Trans. Electron Devices*, vol. 50, pp. 1793–1800, Aug. 2003.

[7] A. Ortiz-Conde, F. J. Garcia Sanchez, M.Guzman, "Exact analytical solution of channel surface potential as an explicit function of gate voltage in undoped-body MOSFETs using the Lambert W function and a threshold voltage definition Therefrom," *Solid-State Electron.*, vol. 47, pp. 2067–2074, 2003.

[8] W. Shangguan, X. Zhou, K. Chandrasekaran, Z. Zhu, S. C. Rustagi, S. B. Chiah, and G. H. See, "Analytical surface-potential solution for generic undoped MOSFETs with two gates," submitted for publication.

[9] X. Zhou, S. B. Chiah, K. Chandrasekaran, G. H. See, W. Shangguan, S. M. Pandey, M. Cheng, S. Chu, and L.-C. Hsia, "Unified regional charge-based versus surface-potential-based compact modeling approaches," *Proc. NSTI Nanotech 2005*, Anaheim, May, 2005, vol. WCM, pp. 25–30.

[10] H. C. Pao and C. T. Sah, "Effects of diffusion current on characteristics of metal-oxide (insulator)-semiconductor transistors," *Solid-State Electron.*, vol. 9, no. 10, pp. 927–937, 1966.

[11] J. W. Sleight and R. Rios, "A continuous compact MOSFET model for SOI with automatic transitions between fully and partially-depleted device behavior," *IEDM Tech. Dig.*, 1996, pp. 143–146.

[12] Y. S. Yu, S. H. Kim, S. W. Hwang, and D. Ahn, "All-analytic surface potential model for SOI MOSFETs," *IEE Proc. - Circuits, Devices and Systems*, vol. 152, no. 2, pp. 183–188, Apr. 2005.

[13] R. van Langevelde and F. M. Klaassen, "An explicit surface-potential-based MOSFET model for circuit simulation," *Solid-State Electron.*, vol. 44, pp. 409–418, 2000.

[14] S. B. Chiah, X. Zhou, K. Chandrasekaran, W. Z. Shangguan, G. H. See, and S. M. Pandey, "Single-piece polycrystalline silicon accumulation/depletion/inversion model with implicit/explicit surface-potential solutions," *Appl. Phys. Lett.*, vol. 86, no. 20, 202111, May 2005.